Electron Transfer in Flavocytochrome P450 BM3: Kinetics of Flavin Reduction and Oxidation, the Role of Cysteine 999, and Relationships with Mammalian Cytochrome P450 Reductase†

Olivier Roitel, Nigel S. Scrutton, and Andrew W. Munro*

Department of Biochemistry, University of Leicester, The Adrian Building, University Road, Leicester LE1 7RH, United Kingdom

Received April 8, 2003; Revised Manuscript Received July 21, 2003

ABSTRACT: Cys-999 is one component of a triad (Cys-999, Ser-830, and Asp-1044) located in the FAD domain of flavocytochrome P450 BM3 that is almost entirely conserved throughout the diflavin reductase family of enzymes. The role of Cys-999 has been studied by steady-state kinetics, stopped-flow spectroscopy, and potentiometry. The C999A mutants of BM3 reductase (containing both FAD and FMN cofactors) and the isolated FAD domain are substantially compromised in their capacity to reduce artificial electron acceptors in steady-state turnover with either NADPH or NADH as electron donors. Stopped-flow studies indicate that this is due primarily to a substantially slower rate of hydride transfer from nicotinamide coenzyme to FAD cofactor in the C999A enzymes. The compromised rates of hydride transfer are not attributable to altered thermodynamic properties of the flavins. A reduced enzyme−$NADP^+$ charge-transfer species is populated following hydride transfer in the wild-type FAD domain, consistent with the slow release of $NADP^+$ from the 2-electron-reduced enzyme. This intermediate does not accumulate in the C999A FAD domain or wild-type and C999A BM3 reductases, suggesting more rapid release of $NADP^+$ from these enzyme forms. Rapid internal electron transfer from FAD to FMN in wild-type BM3 reductase releases $NADP^+$ from the nicotinamide-binding site, thus preventing the inhibition of enzyme activity through the accumulation of a stable $FADH_2$−$NADP^+$ charge-transfer complex. Hydride transfer is reversible, and the observed rate of oxidation of the 2-electron-reduced C999A BM3 reductase and FAD domain is hyperbolically dependent on $NADP^+$ concentration. With the wild-type BM3 reductase and FAD domain, the rate of flavin oxidation displays an unusual dependence on $NADP^+$ concentration, consistent with a two-site binding model in which two coenzyme molecules bind to catalytic and regulatory regions (or sites) within a bipartite coenzyme binding site. A kinetic model is proposed in which binding of coenzyme to the regulatory site hinders sterically the release of NADPH from the catalytic site. The results are discussed in the light of kinetic and structural studies on mammalian cytochrome P450 reductase.

The cytochromes P450 are a superfamily of heme-containing monooxygenase enzymes found in all major domains of life. They catalyze the reductive scission of dioxygen and generate an oxygenated product, water, and $NADP^+$ (*1*). The diflavin reductase enzyme cytochrome P450 reductase (CPR)[1] supplies electrons to eukaryotic P450 enzymes (*2*). CPR has arisen by the fusion of ancestral domains related to flavodoxin and $NADP^+$−ferredoxin oxidoreductase (*3*). Flavocytochrome P450 BM3 comprises a prokaryotic CPR and a soluble P450 (*4*). The reductase of flavocytochrome P450 BM3 is fused to a P450 fatty acid hydroxylase, and the enzyme has high levels of activity toward a range of long-chain fatty acid substrates (*5*); turnover with arachidonic acid is rapid and greater than 15000 per minute (*6*). The crystallographic structure of the heme domain of P450 BM3 has been solved in the presence and absence of bound substrate (*7*, *8*), and solution studies have clarified the roles of a number of active site residues in substrate binding and catalysis (e.g., refs *6* and *9*). Structural and mechanistic studies of the BM3 reductase domains of flavocytochrome P450 BM3 are less advanced than for the P450 domain.

The primary structure of P450 BM3 reductase is 31.5% identical to that of rat CPR but lacks the membrane anchor found in mammalian enzymes. BM3 reductase is also related to other mammalian diflavin reductases, including methionine synthase reductase (MSR; *10*), the isoforms of nitric oxide synthase (NOS; *11*), and human novel reductase 1 (NR1; *12*). Despite the inferred structural similarities, the thermodynamic properties of BM3 reductase are distinct from human and rabbit CPR, suggesting major differences in the catalytic cycles of the bacterial and mammalian enzymes

† This work was funded by the Biotechnology and Biological Sciences Research Council, the Wellcome Trust, the Lister Institute of Preventive Medicine, and the European Community Improving Human Potential program through a Marie Curie Fellowship under Contract HPMF-CT-2002-01633. N.S.S. is a Lister Institute Research Professor. O.R. is a Marie Curie Research Fellow.

* Author to whom correspondence should be addressed. E-mail: awm9@le.ac.uk. Phone: +44 116 252 3464. Fax: +44 116 252 3369.

[1] Abbreviations: CPR, cytochrome P450 reductase; hq, hydroquinone; MSR, methionine synthase reductase; NMN, nicotinamide mononucleotide; NOS, nitric oxide synthase; NR1, novel reductase 1; ox, oxidized; red, reduced; sq, semiquinone; 2′AMP, adenosine 2′-monophosphate; 2′-phospho-AMP, 2′-phosphoadenosine monophosphate.

10.1021/bi034562h CCC: $25.00
Published on Web 08/16/2003

```
CPRBM3          820  LLPSIRPRYYSISSSPRVDEKQASITVSVVSGEAWSGYG-EYKGIASNYLAELQEG----  874
CPRrat          446  LLPRLQARYYSIASSSKVHPNSVHICAVAVEYEAKSGR- VNKGVATSWLRAKEPAGENG  503
CPRhuman        446  LLPRLQARYYSIASSSKVHPNSVHICAVVVEYETKAGR- INKGVATNWLRAKEPAGENG  503
CPRhousefly     444  LLPRLQPRYYSISSSSKLYPTNVHITAVLVQYETPTGR--VNKGVATSYMKEKNPS---V  497
nNOShuman       1171 QLSLLQPRYYSISSSPDMYPDEVHLTVAIVSYRTRDGEGPIHHGVCSSWLNRIQAD----  1226
eNOShuman       930  QLPLLQPRYYSVSSAPSTHPGEIHLTVAVLAYRTQDGLGPLHYGVCSTWLSQLKPG----  985
iNOShuman       899  QLPILKPRFYSISSSRDHTPTEIHLTVAVVTYHTRDGQGPLHHGVCSTWLNSLKPQ----  954
MSRhuman        471  HLPKLQPRPYSCASSSLFHPGKLHFVFNIVEFLSTATTEVLRKGVCTGWLALLVASVLQP  530
MSRCelegans     448  LLPRLIPRPYSMSS--YEN-RKARLIYSEMEFPATDGRRHSRKGLATDWLNSLRIG----  500
Sulfite         378  LLRPLTPRLYSIASSQAEVENEVHVTVGVVRYDV-EGR--ARAGGASSFLADRVEE----  430
NR1human        375  LIPVIRPRAFSIASSLLTHPSRLQILVAVVQFQTRLKE--PRRGLCSSWLASLDPG---Q  429
                      :  : .* :* :*          .    :             * .: ::

CPRBM3          969  ---NQPKTYVQHVME-QDGKKLIELL-DQ-GAHFYICGDGSQMAPAVEATLMKSYADVHQ  1022
CPRrat          599  ----AHKVYVQHLLK-RDREHLWKLIHEG-GAHIYVCGDARNMAKDVQNTFYDIVAEFGP  652
CPRhuman        599  ----SHKVYVQHLLK-QDREHLWKLI-EG-GAHIYVCGDARNMARDVQNTFYDIVAELGA  651
CPRhousefly     593  ----QEKIYVTHLIE-QDADLIWKVIGEQ-KGHFYICGDAKNMAVDVRNILVKILSTKGN  646
nNOShuman       1322 ---DKPKKYVQDILQEQLAESVYRALKEQ-GGHIYVCGDVT-MAADVLKAIQRIMTQQGK  1376
eNOShuman       1081 ---DNPKTYVQDILRTELAAEVHRVLCLE-RGHMFVCGDVT-MATNVLQTVQRILATEGD  1135
iNOShuman       1050 ---GKPKVYVQDILRQQLASEVLRVLHKE-PGHLYVCGDVR-MARDVAHTLKQLVAAKLK  1104
MSRhuman        643  GEEEAPAKYVQDNIQ-LHGQQVARILLQE-NGHIYVCGDAKNMAKDVHDALVQIISKEVG  700
MSRCelegans     605  ----GER--VQDGLR-KYLDKVLPFLTASTESKIFICGDAKGMSKDVWQCFSDIVASDQG  657
Sulfite         522  ----KEKVYVQDKLR-EQGAELWRWI-ND-GAHIYVCGDANRMAKDVEQALLEVIAEFGG  574
NR1human        519  ----EQKVYVQHRLR-ELGSLVWELLDRQ-GAYFYLAGNAKSMPADVSEALMSIFQEEGG  572
                           * . :.      :   :     . :::.*:   *.  *   .

CPRBM3          1023  VSEADARLWLQQLEEKGRYAKDVWAG----------------------------------  1045
CPRrat          653   MEHTQAVDYVKKLMTKGRYSLDVWS----------------------------------  677
CPRhuman        652   MEHAQAVDYIKKLMTKGRYSLDVWS----------------------------------  676
CPRhousefly     647   MNESDAVQYIKKMEAQKRYSADVWS----------------------------------  671
nNOShuman       1377  LSAEDAGVFISRMRDDNRYHEDIFGVTLRTYEVTNRLRSESIAFIEESKK-DTDEVFSS-  1433
eNOShuman       1136  MELDEAGDVIGVLRDQQRYHEDIFGLTLRTQEVTSRIRTQSFSLQERQLRGAVPWAFDPP  1195
iNOShuman       1105  LNEEQVEDYFFQLKSQKRYHEDIFGAVFPYEAKKDRVAVQPSSLEMSAL-----------  1153
MSRhuman        701   VEKLEAMKTLATLKEEKRYLQDIWS----------------------------------  725
MSRCelegans     658   IPDLEAKKKLMDLKKSDQYIEDVWG----------------------------------  682
Sulfite         575   MDTEAADEFLSELRVERRYQRDVY----------------------------------  598
NR1human        573   LCSPDAAAYLARLQQTRRFQTETWA----------------------------------  597
                      :    .   :       ::  : :
```

FIGURE 1: Amino acid sequence alignment of prokaryotic and eukaryotic diflavin reductases. Alignment of amino acid sequences from CPR-like enzymes in the region of the catalytic triad of residues identified by Kasper and co-workers (*40*). These residues (corresponding to Ser-457, Cys-630, and Asp-675 in the rat CPR and to Ser-830, Cys-999, and Asp-1044 in P450 BM3) are highlighted in the alignment. The sequences aligned are BM3 reductase (CPRBM3), rat CPR (CPRrat), human CPR (CPRhuman), housefly CPR (CPRhousefly), human neuronal nitric oxide synthase reductase (nNOShuman), human endothelial nitric oxide synthase reductase (eNOShuman), human immune nitric oxide synthase reductase (iNOShuman), human methionine synthase reductase (MSRhuman), *Caenorhabditis elegans* methionine synthase reductase (MSRCelegans), *E. coli* (CysJ) sulfite reductase (Sulfite), and human novel reductase 1 (NR1human). Sequence deviation in the triad is observed only for the human NR1 enzyme (*12*). Multiple alignment was performed using the program ClustalW via the European Bioinformatics Institute server (http://www.ebi.ac.uk/clustalw/).

(*13*−*15*). These differences in thermodynamic properties also extend to the other mammalian diflavin reductase enzymes (*16*, *17*). BM3 reductase catalyzes the reduction of nonphysiological and artificial electron acceptors (e.g., cytochrome *c* and ferricyanide) more effectively than its mammalian counterparts. It also reduces its own heme domain at rates in excess of 200 s^{-1} (*18*), which far surpasses the reduction rates of mammalian P450s by their cognate CPRs (*19*). The ability of BM3 reductase to deliver electrons rapidly to its P450 domain is due, in part, to the fast reduction of FAD by NADPH, which is considerably slower in mammalian CPR (*20*). Notwithstanding, several residues known to facilitate FAD reduction by NADPH in mammalian CPRs are conserved in BM3 reductase. These include the catalytic triad identified by Kasper and co-workers in rat CPR, comprising Ser-457, Cys-630, and Asp-675 (*21*) (Figure 1). These are equivalent to Ser-830, Cys-999,[2] and Asp-1044 in BM3 reductase (*22*). The rate of reduction of cytochrome *c* by rat C630A CPR is 50-fold less than with wild-type enzyme (*21*), and the rate of reduction of the flavin cofactors by NADPH is impaired. Cys-630 might destabilize the nicotinamide C4−H bond and/or donate a proton to the N5 atom of FAD during enzyme reduction (*21*). Also, minor differences in the flavin absorption spectrum on titration of wild-type and C630A CPR with NADPH have been taken to indicate a perturbed reduction potential that disfavors hydride transfer from NADPH to FAD in the C630A enzyme (*21*).

Alignment of the available sequences for diflavin reductases indicates that Cys-630 of rat CPR is conserved throughout the family of proteins (Figure 1). The exception is human NR1, for which the rate of hydride transfer (1 s^{-1}) from NADPH to FAD is comparatively slow (*17*). Modeling of the FAD domain of flavocytochrome P450 BM3 using the crystal coordinates of rat CPR (*3*) indicates that Cys-999 likely occupies a position analogous to that of Cys-630 in rat CPR. Given the predicted importance of the conserved cysteine residue in hydride transfer throughout the diflavin reductase family, we have examined the effects of replacing this residue in BM3 reductase (mutant C999A), an enzyme in which hydride transfer is rapid. We show that the rate of FAD reduction is substantially impaired in C999A BM3 reductase and FAD domains, consistent with the analogous

[2] Throughout, this residue in full-length flavocytochrome P450 BM3, its BM3 reductase, and the isolated FAD domain is referred to as Cys-999.

role of Cys-630 of rat CPR. Unlike with mammalian CPR, we demonstrate that the rate of flavin reduction in wild-type BM3 reductase shows saturation behavior with respect to NADPH concentration. However, an unusual dependence on $NADP^+$ concentration is seen for the oxidation of BM3 reductase in stopped-flow kinetic studies. We present a kinetic model consistent with this unusual dependence, which invokes the binding of two coenzyme molecules to BM3 reductase. In this model, the binding of $NADP^+$ to the noncatalytic site hinders the release of NADPH (the product) bound at the catalytic site. The model is consistent with the bipartite binding site for nicotinamide coenzyme seen in the structure of rat CPR (*3*). This unusual kinetic behavior is discussed in relation to similar kinetic models advanced for mammalian CPR, NOS, and the *Mycobacterium tuberculosis* adrenodoxin reductase homologue FprA, in which regulation by a second molecule of coenzyme is observed during flavin reduction by NADPH. Our work reinforces the key role of the conserved cysteine residue in hydride transfer in the diflavin reductase family and demonstrates that the kinetics of flavin reduction/oxidation can be regulated by the occupation of coenzyme in a kinetically distinct, noncatalytic binding site that hinders coenzyme release from the catalytic site. Our work also demonstrates a role for Cys-999 in the binding of $NADP^+$ in the 2-electron-reduced FAD domain and indicates that rapid internal electron transfer to the FMN domain is required to prevent the accumulation of inhibited forms of flavocytochrome P450 BM3 in which a stable $FADH_2-NADP^+$ charge-transfer species is formed.

EXPERIMENTAL PROCEDURES

Materials. Oligonucleotide primers for mutagenesis were synthesized in the Protein and Nucleic Acid Chemistry Laboratory (PNACL) at the University of Leicester. *Dpn*I restriction enzyme and *Pfu* DNA polymerase were purchased from Stratagene (Amsterdam, The Netherlands). All other reagents were purchased from Sigma (Poole, U.K.) and were of the highest grade available.

Site-Directed Mutagenesis. Site-directed mutagenesis was performed using the QuikChange method (Stratagene). Template plasmids for mutagenesis were those used for the expression of the isolated FAD domain and the BM3 reductase domains (*18*, *22*, *23*). Oligonucleotide primers used in the mutagenesis procedure were as follows (mismatches indicated by the underlined bases): C999A forward, 5′ GCGCACTTCTATATTGCCGGAGACGGAAGC 3′; C999A reverse, 5′ GCTTCCGTCTCCGGCAATATAGAAGTGCGC 3′. The mutated genes were completely sequenced to verify that no other mutation had arisen during the mutagenesis procedure.

Expression and Purification of the FAD Domain and BM3 Reductase. Expression of the isolated FAD domain and BM3 reductase was in *Escherichia coli* strains BL21(DE3) and TG1, respectively, as described previously (*22*, *23*). Recombinant cells were broken using a French press (three passes at 950 psi) and by sonication. The FAD domain and BM3 reductase were purified by ammonium sulfate fractionation (0−60% and 30−60%, respectively). Ammonium sulfate pellets were resuspended and dialyzed against 50 mM Tris-HCl buffer, pH 7.0 (buffer A), and applied to a DEAE-Sephacel column equilibrated with the same buffer. Protein was eluted using a linear gradient of KCl (0−500 mM) in buffer A. Fractions containing the FAD domain or BM3 reductase were dialyzed against 50 mM phosphate buffer, pH 7.0 (buffer B), and applied to a 2′,5′ADP−Sepharose column equilibrated with the same buffer. After washing, enzymes were eluted with 25 mM 2′AMP contained in buffer B and then dialyzed exhaustively against buffer B to remove 2′AMP. SDS−PAGE (15%) indicated that both protein samples were pure. The enzyme concentration was determined spectrophotometrically using absorption coefficients at 450 nm of 11300 and 21200 M^{-1} cm^{-1}, respectively, for the FAD domain and BM3 reductase (*18*, *23*).

Steady-State Enzyme Assays. The steady-state activities of wild-type and mutant enzymes using ferricyanide or cytochrome *c* as electron acceptor were determined using a Jasco V-550 UV−visible double beam spectrophotometer. To take account of any nonenzyme-mediated reduction of electron acceptor, assays were performed in the double beam spectrophotometer. The reference cuvette contained the same mix as the sample cuvette, but the same volume of buffer replaced the enzyme. The reaction was initiated by the simultaneous addition of NAD(P)H to both cuvettes.

Cytochrome *c* (horse heart) reduction was measured at 550 nm [$\Delta\epsilon_{550nm(red-ox)} = 22640$ M^{-1} cm^{-1} (*24*)], and (potassium) ferricyanide reduction was monitored at 420 nm ($\Delta\epsilon_{420nm(red-ox)} = 1020$ M^{-1} cm^{-1}). Reactions were performed in 50 mM potassium phosphate buffer, pH 7.0, at 25 °C. With ferricyanide as exogenous electron acceptor, saturating concentrations of NADPH (500 μM) were used. The K_m for NADPH was determined at a fixed, saturating concentration of ferricyanide (1.5 mM). The very high K_m (>3 mM) of both wild-type and mutant BM3 reductase domains for NADH prevented experimental determination of this parameter with ferricyanide as the oxidant. With cytochrome *c* as exogenous electron acceptor, saturating concentrations of NADPH (500 μM) were used. The K_m values for NADPH and NADH were determined at a fixed and saturating concentration of cytochrome *c* (100 μM). Analysis of the competitive inhibition of NADPH-dependent reduction of both wild-type and mutant BM3 reductase domains by $NADP^+$ and of the wild-type FAD domain by 2′AMP was performed as described previously (*21*). Origin software (Microcal) was used in data fitting to derive K_m and k_{cat} values from steady-state assays.

Stopped-Flow Kinetic Studies. Single-turnover stopped-flow kinetic studies of flavin reduction in BM3 reductase and the isolated FAD domain were performed using an Applied Photophysics SX.18 MVR stopped-flow spectrophotometer under anaerobic conditions (<5 ppm of oxygen). Flavin reduction by NADH and NADPH was monitored at 450 nm (i.e., near-maximal absorption for the oxidized flavins). Flavin reduction was rapid for both wild-type BM3 reductase and the isolated FAD domain, necessitating measurements at low temperature (5 °C) to obtain accurate rate determinations. Rates of flavin reduction for mutant proteins were measured at 5 and 25 °C. Measurements were carried out in 50 mM potassium phosphate buffer, pH 7.0. Protein concentration in the reaction cell was 4 and 2 μM for the isolated FAD domain and BM3 reductase, respectively. All buffers were made oxygen-free by evacuation and extensive bubbling with oxygen-free argon before use, and stopped-flow reactions were performed in an anaerobic glovebox (Belle Technology). Prior to stopped-flow studies,

protein samples were fully oxidized by treatment with potassium ferricyanide; excess ferricyanide was removed by rapid gel filtration in the glovebox (Pharmacia PD-10 column). Observed rates of flavin reduction were obtained by the fitting of kinetic transients to conventional single- (for the isolated FAD domain) or double-exponential (for BM3 reductase) functions using Spectrakinetics software (Applied Photophysics) as described in Results.

For studies of electron transfer from the 2-electron-reduced FAD domain and 4-electron-reduced BM3 reductase to $NADP^+$, the isolated wild-type and C999A mutant FAD domain and BM3 reductase enzymes were titrated to the 2- and 4-electron level, respectively, with sodium dithionite. These proteins were then mixed rapidly with buffered $NADP^+$ (0−5 mM). Reaction transients at 450 nm were monophasic and analyzed using a single-exponential expression. Similar studies were performed with the 2-electron-reduced FAD domain and buffered NAD^+ (in the range 0−250 mM). Reaction transients at 450 nm were monophasic and analyzed using a single-exponential expression. The influence of a saturating concentration of a nucleotide analogue (2′AMP; K_i of the wild-type FAD domain for 2′AMP was determined as 1.13 ± 0.30 mM) on reduction of $NADP^+$ by the 2-electron-reduced wild-type FAD domain was determined in the same way. The 2-electron-reduced enzyme was preincubated with 2′AMP (10 mM) and then mixed in the stopped flow with buffered $NADP^+$ (0−250 mM). The concentration of the coenzyme was always at least 10-fold greater than the enzyme concentration in all stopped-flow studies to ensure pseudo-first-order conditions. Analysis of the concentration dependence of reaction rates was performed using Origin software (Microcal) to obtain values for the apparent enzyme−coenzyme dissociation constant, *K*, and the limiting rates of flavin reduction and flavin oxidation. The reaction of wild-type (50 μM) and C999A (30 μM) FAD domains and wild-type 20 μM) and C999A (15 μM) BM3 reductases with NADPH (10-fold excess over protein concentration) was monitored by stopped-flow multi-wavelength absorption using a photodiode array detector and X-scan software (Applied Photophysics Ltd.). Reactions were performed in 50 mM phosphate buffer, pH 7.0, at 25 °C, over 0.3 s after the initial mixing event, and the first spectrum was recorded 2.6 ms after mixing.

Potentiometry. Redox titrations were performed in a Belle Technology glovebox under a nitrogen atmosphere. All solutions were degassed under vacuum with argon. Oxygen levels were maintained at <2 ppm. The protein was applied to a Pharmacia PD-10 desalting column in the anaerobic box, preequilibrated with degassed 100 mM phosphate buffer, pH 7.0, and 10% v/v glycerol (titration buffer), to ensure removal of all traces of oxygen. The protein solutions (typically 25−75 μM in ∼8 mL of titration buffer) were titrated electrochemically according to the method of Dutton (*25*) using sodium dithionite as reductant and potassium ferricyanide as oxidant. Dithionite and ferricyanide were delivered in approximately 2 μL aliquots from concentrated stock solutions (typically 10−50 mM). Mediators were added to facilitate electrical communication between the enzyme and the electrode, prior to titration. Typically, 2 μM phenazine methosulfate, 5 μM 2-hydroxy-1,4-naphthoquinone, 0.5 μM methyl viologen, and 1 μM benzyl viologen were included to mediate in the range between +100 and −480 mV, as described previously (*13*, *15*). The electrode was allowed to stabilize between each addition. Spectra (300−800 nm) were recorded using a Cary UV-50 Bio UV−visible scanning spectrophotometer. The electrochemical potential of the solution was measured using a Hanna pH 211 meter coupled to a Pt/calomel electrode (ThermoRussell Ltd.) at 25 ± 2 °C. The electrode was calibrated using the Fe^{3+}/Fe^{2+} EDTA couple as a standard (+108 mV). A factor of +244 mV was used to correct relative to the standard hydrogen electrode. UV−visible spectra were only affected slightly by an increase in baseline with time, contrary to previous studies with the BM3 FAD domain (*15*). Data manipulation and analysis were performed using Origin software (Microcal). For titration of the wild-type and C999A BM3 reductases, absorbance values at 499 nm (isosbestic point for the FAD oxidized/semiquinone couple) and 600 nm (near the absorption maximum for the blue semiquinone form of flavin) were plotted against potential. For titration of the wild-type and C999A FAD domains, absorbance values at 600 nm were plotted against potential. Data were fitted to eq 1, which

$$A = \frac{a10^{(E-E'_1)/59} + b + c10^{(E'_2-E)/59}}{1 + 10^{(E-E'_1)/59} + 10^{(E'_2-E)/59}} \quad (1)$$

represents a 2-electron redox process derived by extension to the Nernst equation and the Beer−Lambert law, as described previously (*13*, *15*). In this equation, *A* is the total absorbance; *a*, *b*, and *c* are component absorbance values contributed by a flavin in the oxidized, semiquinone, and reduced states, respectively; *E* is the observed potential; and E'_1 and E'_2 are the midpoint potentials for oxidized/semiquinone and semiquinone/reduced couples, respectively.

For redox titrations of the wild-type and C999A BM3 reductase (diflavin) enzymes, data at both 499 and 600 nm were fitted to eq 1, as previously described (*15*). At 499 nm there is negligible absorption contribution from the FAD ox/sq transition over the range −100 to −300 mV in which the FMN redox change occurs, allowing determination of the potential for the FMN ox/hq 2-electron couple. At 600 nm, BM3 reductase contributions are from the FAD flavin as a blue semiquinone species develops (first electron addition) and then decays (second electron addition). Fitting was performed as described in the previous study of the potentiometric properties of the P450 BM3 system. All data generated from these fitting procedures were in close agreement with previous studies (*15*).

RESULTS

Purification and General Properties of the Wild-Type and C999A Mutant Proteins. The C999A BM3 reductase and FAD domain were purified by the same chromatographic procedures developed for the wild-type proteins (*15*). Mutagenesis did not adversely affect expression levels or stability of the enzymes, and mutant proteins were recovered in similar yield to the wild-type BM3 reductase and FAD domain. UV−visible spectroscopy revealed that the C999A proteins had optical properties indistinguishable from those of wild-type, with oxidized flavin absorption maxima at 454 and 381 nm (isolated FAD domain) and 456 and 385 nm (BM3 reductase), suggesting that the electronic environment of the FAD or FMN cofactors is not perturbed by the mutation.

Table 1: Steady-State Kinetic Parameters for Cytochrome *c* Reduction by the P450 BM3 Reductase Domain and the C999A Mutant[a]

	wild-type BM3 reductase			C999A BM3 reductase		
substrate varied	NADPH	cyt *c*	NADH	NADPH	cyt *c*	NADH
k_{cat} (s^{-1})	112 ± 5	109 ± 4	17.2 ± 0.6	22 ± 1	23.5 ± 1.5	$(4.0 \pm 0.2) \times 10^{-1}$
K_m (μM)	7.2 ± 0.3	6.2 ± 0.9	$(1.28 \pm 0.1) \times 10^4$	55.6 ± 0.1	10.7 ± 1.5	$(1.41 \pm 0.13) \times 10^4$
k_{cat}/K_m ($\mu M^{-1}\,s^{-1}$)	15.6 ± 1.3	17.6 ± 3.4	$(1.3 \pm 0.1) \times 10^{-3}$	$(4 \pm 0.3) \times 10^{-1}$	2.2 ± 0.4	$(2.8 \pm 0.4) \times 10^{-5}$
$K_i(NADP^+)$ (μM)	8.2 ± 3			22 ± 7		

[a] Kinetic parameters were determined using both NADPH and NADH as electron donors. The K_m and k_{cat} values for cytochrome *c* (cyt *c*) were determined at a fixed and saturating concentration of NADPH (500 μM). The K_m and k_{cat} values for NADH and NADPH, and the K_i values for $NADP^+$, were determined at a fixed and saturating concentration of cytochrome *c* (100 μM). All reactions were performed in 50 mM potassium phosphate buffer, pH 7.0, at 25 °C. The K_i for $NADP^+$ was determined as described previously (*21*).

Table 2: Steady-State Kinetic Parameters for Ferricyanide Reduction by P450 BM3 Reductase and FAD Domains and Their C999A Mutants[a]

	BM3 reductase wild type (C999A)			BM3 FAD domain wild type (C999A)		
substrate varied	NADPH	$Fe(CN)_6^{3-}$	NADH	NADPH	$Fe(CN)_6^{3-}$	NADH
k_{cat} (s^{-1})	287 ± 9	274 ± 4	ND	360 ± 4	ND	20.5 ± 1.7
	(39.4 ± 1.6)	(41.8 ± 2.1)	(ND)	(23.1 ± 0.7)	(24.5 ± 1.1)	(0.31 ± 0.03)
K_m (μM)	23.9 ± 3.1	21.5 ± 1.7	ND	6.5 ± 1.3	>2000	3026 ± 734
	(95.5 ± 15.2)	(7.3 ± 1.1)	(ND)	(49.4 ± 6.5)	(318 ± 31)	(1880 ± 620)
k_{cat}/K_m ($\mu M^{-1}\,s^{-1}$)	12.0 ± 0.7	12.7 ± 1.5	ND	55.4 ± 11.7	ND	$(7 \pm 2) \times 10^{-3}$
	(0.41 ± 0.08)	(5.72 ± 1.03)	(ND)	(0.47 ± 0.08)	(0.08 ± 0.1)	$((16 \pm 6) \times 10^{-5})$

[a] Kinetic parameters were determined using both NADPH and NADH as electron donors. The K_m and k_{cat} values for ferricyanide [$Fe(CN)_6^{3-}$] were determined at a fixed and saturating concentration of NADPH (500 μM). The K_m and k_{cat} values for NADH and NADPH were determined at a fixed and saturating concentration of ferricyanide (1.5 mM). All reactions were performed in 50 mM potassium phosphate buffer, pH 7.0, at 25 °C. ND: not determined. In the case of ferricyanide reduction by the wild-type FAD domain, increase in reduction rate was linear up to a ferricyanide concentration of 2 mM. Figures in parentheses indicate values of kinetic parameters for the C999A enzymes.

Steady-State Kinetics with Cytochrome c as Electron Acceptor. Kinetic properties of the wild-type and C999A mutant forms of the BM3 reductase for reduction of the nonphysiological electron acceptor cytochrome *c* are reported in Table 1. With NADPH as the reductant (500 μM), the rate of reduction of cytochrome *c* by the C999A BM3 reductase is diminished approximately 5-fold, and the apparent K_m for cytochrome *c* is also increased slightly, leading to a 8-fold decrease in the catalytic efficiency (k_{cat}/K_m) (Table 1). At saturating cytochrome *c*, the apparent K_m for NADPH is increased 7.7-fold in the C999A BM3 reductase. From cytochrome *c* reduction studies with wild-type BM3 reductase, the apparent K_m for NADH is $\sim 10^3$-fold higher than for NADPH (12.8 mM, compared to 7.2 μM for wild-type reductase). The K_m for NADH is not significantly changed in the C999A mutant, but the k_{cat} for cytochrome *c* reduction is 43-fold lower with the C999A enzyme.

We evaluated the effects of the C999A mutation on the affinity for $NADP^+$ (the product of NADPH-dependent flavin reduction) by examining the inhibition of cytochrome *c* reduction by wild-type and C999A BM3 reductase. $NADP^+$ is a competitive inhibitor with respect to NADPH, and the apparent K_i value is $\sim$3-fold higher for C999A BM3 reductase, suggesting that interaction with Cys-999 favors the binding of $NADP^+$ (Table 1).

For wild-type BM3 reductase, the k_{cat} values for cytochrome *c* reduction are within error of those reported previously for the reaction catalyzed by the intact flavocytochrome P450 BM3 (*26*). The apparent K_m values for the NAD(P)H cofactors are slightly higher than those reported previously with intact flavocytochrome P450 BM3 (7.2 ± 0.3 μM, cf. 1.2 ± 0.2 μM for NADPH; 12.8 ± 1.0 mM, cf. 2.7 ± 1.0 mM for NADH) (*26*). Repetition of BM3 reductase cytochrome *c* reductase assays in 50 mM Tris-HCl (7.0) had no significant effect on k_{cat} values but produced slightly lower estimates of K_m values for the pyridine nucleotide cofactors, suggesting some influence of buffer system on nucleotide binding (2.0 ± 0.2 μM for NADPH, 6.0 ± 0.8 mM for NADH).

Steady-State Kinetics with Ferricyanide as Electron Acceptor. Qualitatively, similar effects on the steady-state behavior seen with cytochrome *c* as electron acceptor were also observed when ferricyanide served as electron acceptor (Table 2). Unlike cytochrome *c*, which accepts electrons from the FMN domain of BM3 reductase, ferricyanide can accept electrons from the FAD domain. Thus, kinetic parameters for ferricyanide reduction by wild-type and C999A variants of both BM3 reductase and FAD domains were investigated. The k_{cat} value for ferricyanide reduction was decreased 6.6-fold on replacing Cys-999 by alanine in the BM3 reductase (Table 2). The apparent K_m values for ferricyanide were decreased by factors of >6.3- and 2.9-fold for the C999A FAD domain and BM3 reductase, respectively. The combined effect is to reduce the apparent catalytic efficiency with ferricyanide by 2.2-fold for the C999A BM3 reductase.

In assays performed at a fixed concentration of ferricyanide (1.5 mM), apparent K_m values for NADPH with BM3 reductase are elevated over those for the FAD domain. A further increase in apparent K_m for NADPH is induced by the C999A mutation for both the FAD domain (7.6-fold) and BM3 reductase (4.0-fold). With NADH as the electron donor, the k_{cat} is considerably diminished compared with NADPH by factors of 17.6- and 74.5-fold for wild-type and C999A FAD domains, respectively. The apparent K_m value for NADH is not substantially affected by mutation of Cys-999 to alanine in the FAD domain.

Kinetics of Flavin Reduction. The influence of the C999A mutation on the kinetics of hydride transfer from NAD(P)H to FAD was investigated using stopped-flow methods.

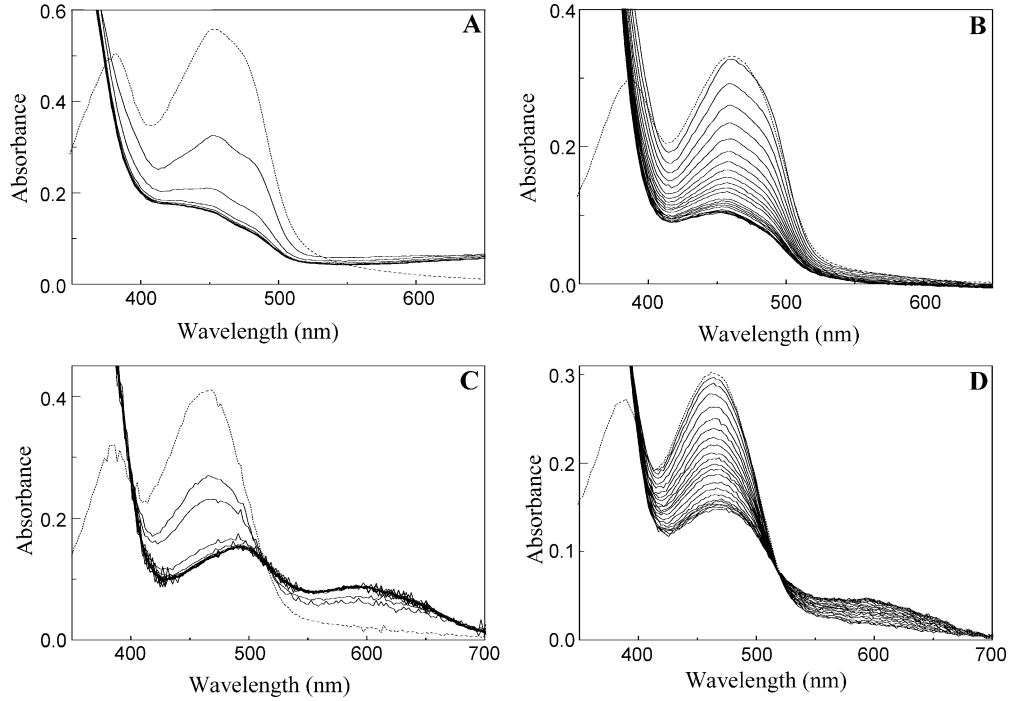

FIGURE 2: Reaction of wild-type and C999A FAD domains with NADPH monitored by stopped-flow photodiode array spectroscopy. The reaction of wild-type (50 μM) and C999A (30 μM) FAD domains and wild-type (20 μM) and C999A (15 μM) BM3 reductase domains with NADPH (500, 300, 200, and 150 μM, respectively) was monitored by stopped-flow multiwavelength absorption using a photodiode array detector and X-scan software (Applied Photophysics Ltd.). Reactions were performed in 50 mM phosphate buffer, pH 7.0, at 25 °C, over 0.3 s after the initial mixing event, and the first spectrum was recorded 2.6 ms after mixing. For clarity, only selected subsequent spectra are shown. The spectrum of the oxidized enzyme is indicated by a dotted line. Panels: (A) wild-type FAD domain; (B) C999A FAD domain; (C) wild-type BM3 reductase; (D) C999A BM3 reductase. For the wild-type FAD domain and BM3 reductase (panels A and C), the reaction is completed rapidly, and postmixing spectra (at approximately 2.6 ms intervals) between 0 and 12.8 ms and between 0 and 18.0 ms, respectively, are shown. For the C999A FAD domain and BM3 reductase (panels B and D), the reactions are slower, and spectra recorded at regular intervals between 0 and 300 ms are shown in both cases. Formation of the neutral blue semiquinone is observed for the BM3 reductase domain spectra (panels C and D). A charge-transfer band at long wavelength is observed only in the case of the wild-type FAD domain (panel A).

Reduction of wild-type BM3 reductase and the FAD domain occurs rapidly (>500 s^{-1}) at 25 °C, preventing the precise determination of rates using the stopped-flow method, but by reducing the temperature to 5 °C the reductive transients were readily analyzed. The rates of flavin reduction were considerably slower for the C999A BM3 reductase and FAD domain, allowing the acquisition of reaction transients at 25 °C. Prior to detailed stopped-flow studies performed at a single wavelength, we performed a series of experiments using photodiode array detection. Reduction of the wild-type FAD domain was accompanied by the development of a characteristic absorption feature at long wavelength (Figure 2, panel A), which we attribute to the formation of a $FADH_2-NADP^+$ charge-transfer species. Similar species have been observed with other flavoproteins (e.g., ref *27*). This charge-transfer species is not present in similar reactions of the C999A FAD domain, suggesting that the binding of $NADP^+$ to the 2-electron-reduced form of this domain is weaker. Also, photodiode array experiments performed with wild-type and C999A BM3 reductase indicate that the charge-transfer species does not form and that spectral features indicating the formation of a blue semiquinone species are formed following FAD reduction. The formation of the blue semiquinone is the result of inter-flavin electron transfer from $FADH_2$ to FMN to generate the diradical form of the enzyme ($FADH^{\bullet}/FMNH^{\bullet}$), as described previously (*26*). Consequently, the $FADH_2-NADP^+$ charge-transfer species does not accumulate, and $NADP^+$ is released from the FAD domain; this prevents the accumulation of a kinetic bottleneck in steady-state turnover of flavocytochrome P450 BM3.

In single-wavelength studies at 450 nm, kinetic transients were monophasic for reduction of the FAD domains and biphasic for the BM3 reductases. For the BM3 reductases, the rate of the slower second phase was independent of the concentration of reducing coenzyme (Table 3), and this phase contributed ~20% of the total absorption change at 450 nm.[3] The first kinetic phase reports on flavin reduction by NADPH, and the observed rate for this phase shows a hyperbolic dependence on the concentration of NADPH (Table 3). The observed rate for flavin reduction with the FAD domains was likewise hyperbolically dependent on coenzyme concentration (Table 3), allowing estimation of the limiting rates for hydride transfer (k_{lim}) by fitting to a general hyperbolic equation (eq 2). Analysis of the rates of

$$k_{obs} = k_{lim}[S]/(K + [S]) \quad (2)$$

flavin reduction and oxidation (see below) in this way indicates that the k_{lim} values are roughly equal for the reductive and oxidative reactions in the C999A BM3

[3] The origin of this absorption change is uncertain. It might be associated with internal electron transfer between the flavins, or conformational change that affects the absorption of the flavins, as the reductase approaches its most thermodynamically stable state.

Table 3: Rate Constants and Apparent Enzyme−Coenzyme Dissociation Constants Obtained from Analysis of Stopped-Flow Kinetic Data for Wild-Type and C999A Mutants of BM3 Reductase and FAD Domains[a]

	BM3 reductase		BM3 FAD domain	
	wild type	C999A	wild type	C999A
k_{lim}^{NADPH} (s^{-1})	238 ± 6 (61 ± 3)	23.2 ± 0.3 (0.35 ± 0.05)	364 ± 25	15.9 ± 0.3
K^{NADPH} (μM)	35 ± 3	74 ± 3	23 ± 6	22.9 ± 1.8
k_{lim}^{NADH} (s^{-1})	4.3 ± 0.1 (0.10 ± 0.02)	0.23 ± 0.02 (0.07 ± 0.01)	6.9 ± 0.2	0.42 ± 0.01
K^{NADH} (mM)	26.3 ± 2.2	38 ± 7	10.9 ± 1.0	33.7 ± 1.8
k_{lim}^{NADP} (s^{-1})	ND	22.7 ± 0.8	ND	16 ± 2
K^{NADP} (μM)	ND	46 ± 5	ND	0.70 ± 0.22

[a] All reactions were performed in 50 mM potassium phosphate, pH 7.0, at 5 and 25 °C, for wild-type and mutant enzymes, respectively, as indicated in Experimental Procedures. In stopped-flow experiments involving rapid mixing of oxidized enzyme with reducing coenzyme, values for the limiting rate constants for flavin reduction ($k_{lim}^{NAD(P)H}$) and apparent dissociation constants ($K^{NAD(P)H}$) were determined by fitting to eq 2. For the wild-type and C999A forms of BM3 reductase, rate constants for the slow phase of the biphasic transient are also given in parentheses. This slow phase is independent of the coenzyme concentration. In stopped-flow experiments involving rapid mixing of reduced enzyme with $NADP^+$, values for the limiting rate constant for flavin oxidation (k_{lim}^{NADP}) and the apparent reduced enzyme−$NADP^+$ dissociation constant (K^{NADP}) were also determined for C999A enzymes by fitting to eq 2. In the case of the wild-type BM3 reductase and FAD domains, these values were not determinable (ND) due to the inverted dependence of oxidation kinetics on [$NADP^+$]. The flavin oxidation rate at the lowest [$NADP^+$] tested (1.5 × that of the [enzyme]) was approximately 18−19 s^{-1} for both the wild-type FAD domain and BM3 reductase (see Figure 3).

reductase and FAD domain reactions with $NADP^+$(H). The true wild-type BM3 reductase and FAD domain k_{lim} values for flavin reoxidation with $NADP^+$ are not determinable due to acceleration of the rate as [$NADP^+$] is lowered (see below), but the rates observed are generally much slower than for the reductive reactions with NADPH (Table 3). This is in contrast to mammalian CPR, where the reverse reaction proceeds at a faster rate (*20*). In the case of mammalian CPR it has been suggested that this reflects the evolutionary origins of the CPR FAD domain, whose structure resembles that of ferredoxin−$NADP^+$ reductase (FNR). FNR functions to reduce $NADP^+$ in the cell and thus transfers electrons in the opposite direction to CPR and BM3 reductase.

To facilitate direct comparison of the rates of flavin reduction between wild-type and C999A enzymes, the kinetics of flavin reduction in the C999A FAD domain were also determined at 5 °C. As expected, the limiting rate constant for flavin reduction, k_{lim}, was decreased for the C999A FAD domain from 15.9 ± 0.3 s^{-1} (25 °C) to 4.85 ± 0.05 s^{-1} (5 °C). This compares with a value of 364 ± 25 s^{-1} at 5 °C for the wild-type FAD domain. The value of K for NADPH in the C999A FAD domain is 13.5 ± 1.0 μM at 5 °C, indicating the absence of major temperature effects on this parameter. A full comparison of kinetic data for wild-type (5 °C) and C999A (25 °C) FAD domains and BM3 reductases, in reactions with NADPH and NADH, is presented in Table 3. Only modest changes (∼2-fold) are seen in the value of K for the reaction of wild-type and C999A BM3 reductase with NADPH, suggesting little effect on the binding of NADPH to the oxidized enzyme. The major effect of the mutation is to diminish the limiting rate constant for flavin reduction by approximately 1 order of magnitude. Combined, these data reveal that a major role of Cys-999 is to facilitate hydride transfer from NADPH to FAD, which is consistent with the function of Cys-630 in rat CPR (*21*). The lack of a major effect on K following mutation suggests Cys-999 does not have a major role in the binding of NADPH, but steady-state data (see above; Table 1) and stopped-flow photodiode array data (Figure 2A) suggest a role in binding the product ($NADP^+$).

Corresponding studies with NADH indicated that the limiting rate constants for flavin reduction were substantially compromised in the C999A enzymes (Table 3). Additionally, the kinetic parameter K was elevated by a factor of approximately 750-fold and 510-fold, respectively, for wild-type and C999A BM3 reductase enzymes compared with data collected using NADPH. There is a modest increase (∼3-fold) in K for reaction of the C999A FAD domain with NADH compared to the wild-type FAD domain (Table 3). Although the limiting rate constant for flavin reduction is compromised in reactions of the C999A enzymes with NADH, the extent is less than that observed with NADPH. This implies that the geometry for hydride transfer from NADH to FAD in wild-type and C999A enzymes is less optimal than with NADPH, which accounts for the decreased flavin reduction rates with NADH and the smaller compromising effect on mutating Cys-999 relative to those reactions performed with NADPH.

Kinetics of Flavin Oxidation by $NADP^+$ in C999A Enzymes. We have also investigated the reversibility of hydride transfer using stopped-flow methods. Wild-type and C999A FAD domains were reduced with dithionite at the 2-electron level prior to rapid mixing with $NADP^+$. Similarly, wild-type and C999A BM3 reductases were reduced with dithionite at the 4-electron level and then mixed in the stopped-flow instrument with $NADP^+$. Kinetic transients were monophasic and analyzed using a single-exponential function. For the C999A FAD domain and BM3 reductase, the rate of flavin oxidation was hyperbolically dependent on the concentration of $NADP^+$ and approached limiting values at high $NADP^+$ concentration (Table 3; Figure 3B,D). The value of the limiting rate constant for flavin oxidation, k_{lim}, for C999A BM3 reductase is slightly elevated (∼1.5-fold) compared with the C999A FAD domain. The 2-electron-reduced C999A FAD domain has a much stronger affinity (∼65-fold) for $NADP^+$ compared with C999A BM3 reductase (Table 3). The origin of this differential affinity is unclear.

Kinetics of Flavin Oxidation by $NADP^+$ in Wild-Type Enzymes. For the wild-type FAD domain and BM3 reductase, the observed rate of flavin oxidation showed an unusual dependence on the concentration of $NADP^+$ (Figure 3A,C). The type of inverse rate dependence on nicotinamide coenzyme concentration exhibited by the wild-type FAD and BM3 reductase domains has been observed previously for the reduction by NADPH of human CPR (*20*), rat neuronal nitric oxide synthase (*28*), and the adrenodoxin reductase homologue FprA from *M. tuberculosis* (*29*). In each case, the increased flavin reduction rates observed at low NADPH concentration were rationalized in terms of two kinetically distinct binding sites for pyridine nucleotide, one catalytic and one regulatory. Population of the regulatory binding site was proposed to decrease the rate of flavin reduction for

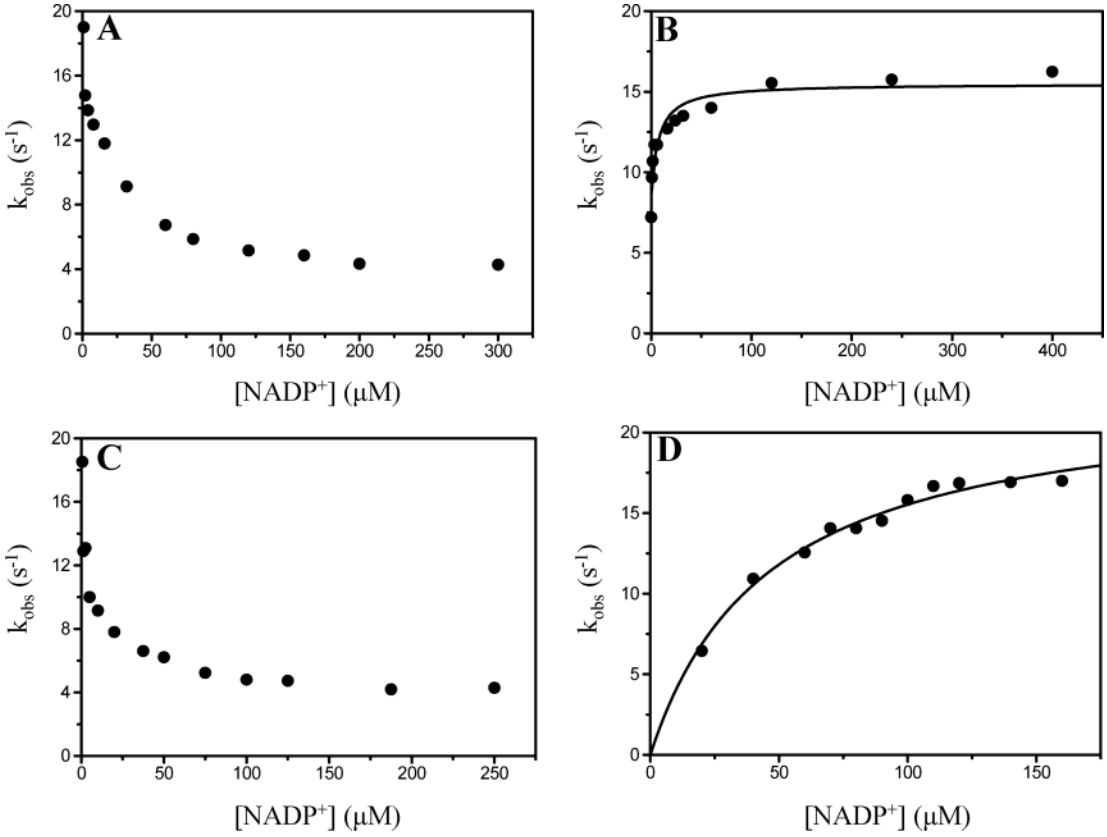

FIGURE 3: Dependence of the observed rates of flavin oxidation on NADP$^+$ concentration for the wild-type and C999A mutant FAD and BM3 reductase domains of P450 BM3. Hydride transfer from the 2-electron-reduced FAD (4 μM) and 4-electron-reduced BM3 reductase (2 μM) domains to NADP$^+$ (in the range 0−0.5 mM) was monitored by absorption stopped-flow experiments at 450 nm, as indicated in Experimental Procedures. Measurements were carried out in 50 mM potassium phosphate buffer, pH 7.0, at 5 and 25 °C, for the wild-type and C999A enzymes, respectively. A single-exponential process described all reaction transients, and observed rates were calculated using Spectrakinetics software (Applied Photophysics). Panels: (A) wild-type FAD domain; (B) C999A FAD domain; (C) wild-type BM3 reductase domain; (D) C999A BM3 reductase domain.

coenzyme bound in the catalytic site by hindering the dissociation of NADP$^+$ from the catalytic site (*30*; and see later for detailed discussion). We suggest a similar mechanism applies for the oxidation of the wild-type FAD domain and BM3 reductase. In this case, the binding of NADP$^+$ to a kinetically distinct and noncatalytic site hinders the release of the NADPH product from the catalytic site following hydride transfer from the flavin. To investigate this proposal further, additional studies were performed. First, the wild-type FAD domain was reduced at the 2-electron level with dithionite and then mixed with NAD$^+$. In a second experiment, the reduced wild-type FAD domain was preincubated with 2′AMP (10 mM) prior to mixing with NADP$^+$. In both cases, the reoxidation kinetics displayed a hyperbolic dependence on coenzyme concentration (Figure 4). This contrasts with the inverted dependence of the flavin oxidation rate as a function of coenzyme concentration observed for the wild-type FAD domain with NADP$^+$ in the absence of the 2′AMP (Figure 3) and is consistent with a dual binding site model (Figure 5). With NAD$^+$, the lack of a 2′-phosphate moiety impairs binding at the noncatalytic site, and thus release of NADH product from the catalytic site is not affected. In reactions performed with NADPH and 2′AMP, the latter is bound at the regulatory site. However, the smaller size of 2′AMP compared with NADPH allows the release of NADPH from the catalytic site without steric hindrance. We propose that the catalytic site is analogous to the NMN-binding region of the structurally defined coenzyme-binding site in rat CPR (*3*) and that the regulatory site is analogous to the region of the rat CPR coenzyme-binding site that interacts with the 2′-phospho-AMP moiety of the NADP$^+$(H) cofactor. The bipartite recognition of nicotinamide coenzyme in the BM3 reductase family is therefore consistent with our proposed kinetic model. In this model, the binding of NADP$^+$, through its 2′-phospho-AMP moiety in the regulatory site, hinders sterically the release of NADPH from the catalytic site, which is bound primarily through its NMN moiety (Figure 6).

Potentiometry of Wild-Type and C999A Enzymes. Given the substantially compromised flavin reduction rates observed in the C999A BM3 reductase and isolated FAD domain, we determined the reduction potentials for the flavin cofactors in wild-type and C999A proteins to search for any thermodynamic origin in the observed reaction kinetics. By using the highly purified FAD domain of BM3, protein precipitation noted previously for this domain at negative potentials did not occur (*15*). As a result, spectral data collected for the FAD domains at low potentials were of higher quality than those obtained previously, leading to improved fitting of data and considerably reduced errors (Figures 7 and 8). Notwithstanding these improvements in data quality, midpoint reduction potentials for the wild-type FAD domain were within error of those determined previously (E_{12} = −320 ± 4 mV compared to −303 ± 15 mV from the previous study), and the relevant values for the FAD cofactor in the wild-type reductase domain are essentially identical

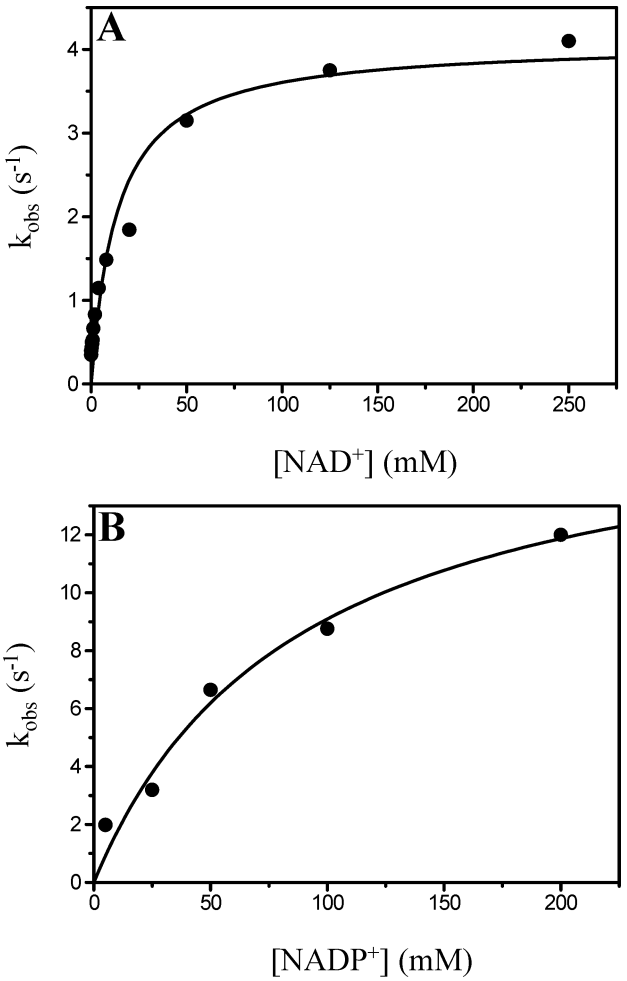

FIGURE 4: Dependence of the observed rates of flavin oxidation on NAD^+ and $NADP^+$ concentration for the wild-type BM3 FAD domain and for the wild-type BM3 FAD domain preincubated with adenosine 2′-monophosphate. Hydride transfer from the 2-electron-reduced wild-type FAD domain (4 μM) to NAD^+ (in the range 0−250 mM) (panel A) and from the 2-electron-reduced wild-type FAD domain (4 μM) preincubated with 10 mM adenosine 2′-monophosphate to $NADP^+$ (in the range 0−250 mM) (panel B) was monitored by absorption stopped-flow spectroscopy at 450 nm, as indicated in Experimental Procedures. Measurements were carried out in 50 mM potassium phosphate buffer, pH 7.0, at 5 °C. Observed rates were calculated using Spectrakinetics software (Applied Photophysics). Control experiments in which potassium chloride was added up to 200 mM indicated that elevated ionic strength due to the required high pyridine nucleotide concentrations had no significant effect on the flavin oxidation rates measured.

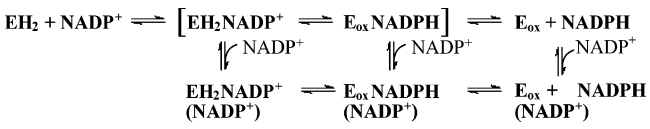

FIGURE 5: Reaction scheme for hydride transfer from the 2-electron-reduced wild-type FAD domain to $NADP^+$. Oxidized (E_{ox}) and reduced (EH_2) forms of the FAD domain of the enzyme interact with either NADPH or $NADP^+$ cofactors, which can bind to the catalytic and regulatory binding sites. In the reaction shown in this scheme, occupation of the regulatory site is indicated by $NADP^+$ in parentheses. Binding of $NADP^+$ to the regulatory site hinders sterically the release of NADPH from the catalytic site, thus attenuating the rate of formation of E_{ox}.

($E_{12} = -330 \pm 4$ mV compared to -332 ± 4 mV from the previous study; Table 5). Values for the C999A mutants of the FAD and reductase domains were not significantly

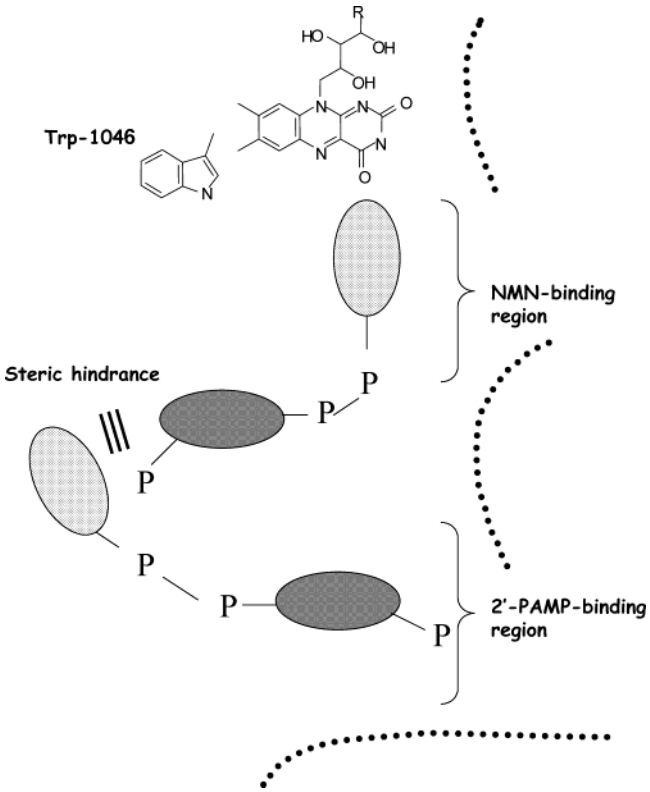

FIGURE 6: Proposed model for binding of catalytic and inhibitory NADP(H) molecules in the bipartite coenzyme-binding site in BM3 reductase. Cartoon illustrating the proposed two-site binding model in which the 2′-phospho-AMP (2′-PAMP) moiety of the regulatory coenzyme competes with the adenosine moiety of the catalytic coenzyme for the common 2′-phospho-AMP-binding site in the structurally identified (for rat CPR) bipartite coenzyme-binding site. The 2′-phospho-AMP moieties of each coenzyme are shown as densely filled ellipsoids, and the NMN moieties are shown as lightly filled ellipsoids. Dotted lines indicate the protein surface forming the bipartite coenzyme-binding site. The NMN moiety of the regulatory coenzyme sterically interferes with the release of NADPH (the catalytic coenzyme molecule formed following hydride transfer from the FAD). At coenzyme concentrations equal to the enzyme concentration, the adenosine moiety of the catalytic coenzyme binds to the 2′-phospho-AMP-binding region of the bipartite binding site in the absence of competition from a regulatory coenzyme molecule, and the release of NADPH is not hindered sterically following hydride transfer from the FAD.

changed from the values for the wild-type enzymes ($E_{12} = -335 \pm 3$ and -333 ± 4 mV, respectively), indicating that the overall driving force for electron transfer to the FAD cofactor is not significantly perturbed by the mutation. The slightly more negative 2-electron couple determined for the C999A FAD domain compared to the wild-type domain is due largely to the more negative semiquinone/hydroquinone (E_2) couple in this case: -400 ± 4 mV compared to -375 ± 4 mV (Table 5). However, since the relevant couples are virtually identical in the FAD cofactors of wild-type and C999A BM3 reductase domains, thermodynamic effects do not account for the impaired rates of hydride transfer in the C999A mutants.

DISCUSSION

The BM3 reductase domain of flavocytochrome P450 BM3 was the first characterized prokaryotic CPR (*4*) and is fused to the P450 domain in a fashion similar to the eukaryotic nitric oxide synthases (*31*). Genome sequencing

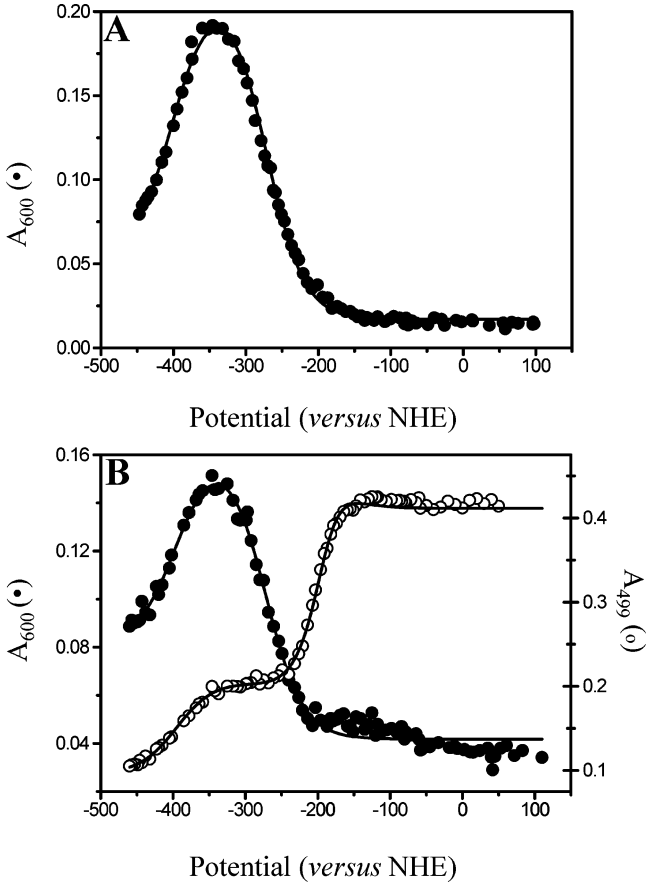

FIGURE 7: Absorbance versus potential plots for the C999A FAD and C999A reductase domains of P450 BM3. Panel A: For the C999A FAD domain, plot of A_{600} (filled circles; absorption near the blue semiquinone maximum) versus reduction potential fitted to a 2-electron Nernst function, as described in Experimental Procedures. Midpoint reduction potentials for the FAD ox/sq (−271 ± 3 mV) and FAD sq/hq (−400 ± 3 mV) couples were determined from the data fit. Panel B: For the C999A reductase domain, plot of absorbance versus reduction potential at 499 nm (open circles; at this wavelength there is negligible absorption contribution from the FAD ox/sq transition over the range −100 to −300 mV in which the FMN redox change occurs, right axis) and 600 nm (filled circles; near the blue semiquinone maximum, left axis) fitted to a 2-electron Nernst function, as described in Experimental Procedures. From the 499 nm data, the midpoint reduction potential for the FMN ox/hq 2-electron couple is −192 ± 10 mV. From the 600 nm data, the midpoint reduction potentials for the FAD single electron couples are ox/sq (−272 ± 3 mV) and sq/hq (−395 ± 5 mV).

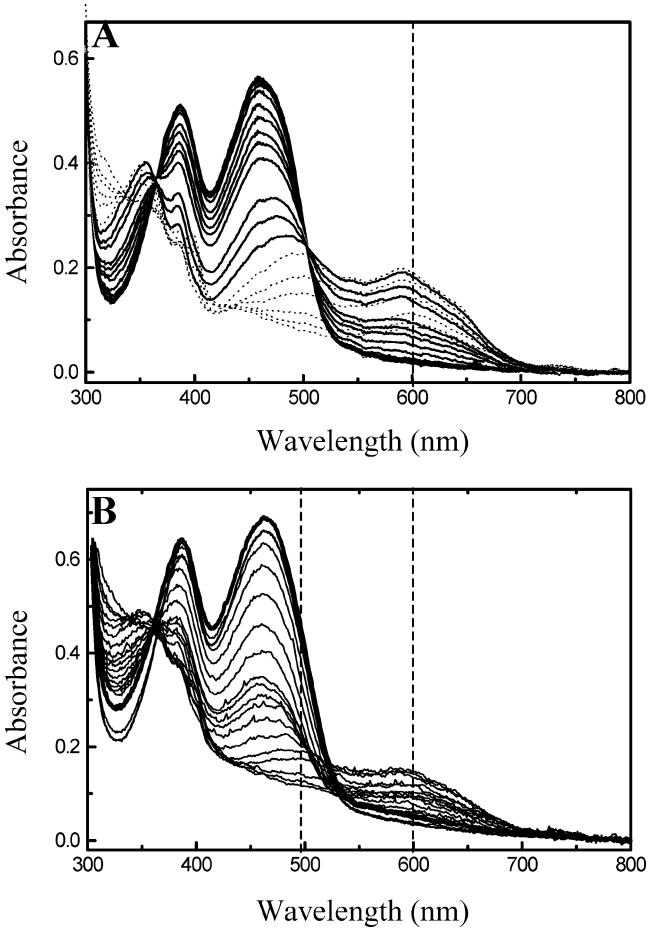

FIGURE 8: Spectral changes during redox titrations of the C999A mutants of the P450 BM3 FAD and reductase domains. Anaerobic spectroelectrochemical titrations of the C999A FAD (panel A) and C999A BM3 reductase (panel B) domains of P450 BM3 were performed as described in Experimental Procedures. Approximately 100 spectra were collected across the relevant range of potentials. For clarity, only selected spectra are shown. The highest intensity spectra are those of the oxidized C999A FAD (panel A) and C999A BM3 reductase domain (panel B) and are shown as thick solid black lines. For the FAD domain, thin solid black lines indicate spectra recorded during the addition of the first electron (oxidized to semiquinone transition), whereas dotted lines show spectra recorded during addition of the second electron (semiquinone to hydroquinone transition). Vertical dotted lines indicate the wavelengths for which data were collected to calculate midpoint reduction potentials: 600 nm (FAD and BM3 reductase) and 499 nm (BM3 reductase).

projects have revealed the presence of two BM3 homologues in *Bacillus subtilis* (CYPs 102A2 and 102A3) (*32*, *33*) and in the heavy metal tolerant bacterium *Ralstonia metallidurans* (*34*), so the diversity of these fusion proteins is evident, although precise physiological roles remain obscure. The bacterial CPRs lack the N-terminal membrane anchor found in eukaryotic CPRs, and the reductase domain of BM3 is a soluble enzyme that can be expressed to high levels in *E. coli* (*23*). However, despite inferred structural similarities, the thermodynamic properties of the BM3 reductase are distinct from those of mammalian diflavin reductases, such as CPR and NOS. In mammalian diflavin reductases, the FMN semiquinone is stabilized with respect to the hydroquinone (*13*, *35*), but this is not the case with the FMN domain of BM3 reductase (*15*). In redox titrations of BM3 reductase and its FMN domain, the neutral, blue semiquinone form of the FMN is not populated. By contrast, the eukaryotic CPRs (including rabbit, rat, and human forms) are purified in a 1-electron-reduced form, in which the FMN is reduced to an air-stable semiquinone species (e.g., ref *13*). Despite the differences in electronic properties of the FMN cofactor, the FAD in BM3 behaves like the FAD in eukaryotic enzymes, in that it stabilizes a blue semiquinone form during redox titrations. Residues considered important for catalysis in the mammalian forms of CPR are also conserved in BM3 CPR, including the catalytic triad of residues formed by Ser-830, Cys-999, and Asp-1044.

Herein, we have demonstrated the importance of Cys-999 in the reductive and oxidative reactions of BM3 reductase and the isolated FAD domain. In the C999A enzyme, limiting rate constants for hydride transfer are diminished considerably with NADPH (73.4-fold with the FAD domain under identical conditions), consistent with similar studies on the

Table 4: Rate Constants and Apparent NAD(P)$^+$-Reduced Enzyme Dissociation Constants Obtained from Analysis of Stopped-Flow Kinetic Data for Wild-Type FAD Domains with NAD^+ or $NADP^+$ and 2′AMP[a]

enzyme	K_{lim}^{NAD} (s^{-1})	K^{NAD} (mM)	$K_{lim}^{2'AMP\cdot NADP}$ (s^{-1})	$K^{2'AMP\cdot NADP}$ (mM)
FAD domain	4.0 ± 0.3	13.5 ± 3.6	17.1 ± 2.5	87.9 ± 28.2

[a] Reactions were performed in 50 mM potassium phosphate, pH 7.0, at 5 °C, as described in Experimental Procedures. The wild-type FAD domain was reduced at the 2-electron level by titration with sodium dithionite prior to rapid mixing with NAD^+. The corresponding rate and dissociation constants (k_{lim}^{NAD} and K^{NAD}) were determined by fitting the data to eq 2. The wild-type FAD domain reduced at the 2-electron level and incubated with 10 mM 2′AMP was also mixed rapidly with $NADP^+$. The corresponding rate and dissociation constants ($k_{lim}^{2'AMP\cdot NADP}$ and $K^{2'AMP\cdot NADP}$) were also determined by fitting the data to eq 2.

Table 5: Midpoint Reduction Potentials [E' (mV versus NHE)] for FAD and FMN Cofactors in Wild-Type and C999A Mutant P450 BM3 Reductase and FAD Domains[a]

enzyme	E'_{12}	E'_1	E'_2
FAD domain	-320 ± 4	-264 ± 3	-375 ± 4
BM3 reductase FAD	-330 ± 4	-276 ± 3	-384 ± 5
BM3 reductase FMN	-203 ± 5	ND	ND
C999A FAD domain	-335 ± 3	-271 ± 3	-400 ± 4
C999A reductase FAD	-333 ± 4	-272 ± 3	-395 ± 5
C999A reductase FMN	-192 ± 10	ND	ND

[a] Potentials were determined from plots of electrode potential versus absorbance data as described in Experimental Procedures. All values were derived from titrations performed with 100 mM phosphate buffer, 10% v/v glycerol, pH 7.0, at 25 ± 2 °C. E'_{12} refers to $F_{ox} + 2e^- \leftrightarrow F_{red}$; E'_1 refers to $F_{ox} + e^- \leftrightarrow F_{sq}$; E'_2 refers to $F_{sq} + e^- \leftrightarrow F_{red}$ (F ≡ flavin, e^- ≡ electron, ox ≡ oxidized, sq ≡ semiquinone, and red ≡ reduced). ND: not determinable since E'_2 for the FMN cofactor is more positive than E'_1 , resulting in an apparent concerted 2-electron conversion between oxidized and reduced forms on reduction, with no formation of a semiquinone intermediate.

C630A rat CPR (*21*). However, hydride transfer is considerably faster with the BM3 domains compared to mammalian CPR. As with human CPR (*20*), hydride transfer is reversible in BM3 reductase and the FAD domain (*36*). This is consistent with previous proposals that rapid transfer of 1 electron from FAD to FMN is a key factor in controlling the direction of electron transfer in P450 BM3. Thus, thermodynamic analysis of P450 BM3 indicates that during turnover one or both electrons on the FAD should be transferred to the more positive potential FMN cofactor, and this will suppress the reverse hydride transfer reaction to $NADP^+$ (*13*, *20*, *30*).

Murataliev and Feyereisen have considered the importance of $NADP^+$ release as the rate-limiting step in catalysis with housefly CPR (*20*, *37*), and this is likely also to be true for electron transfer through BM3 reductase. Our stopped-flow work with the isolated FAD domain indicates that the $FADH_2-NADP^+$ charge-transfer species is relatively stable. In steady-state assays with ferricyanide, oxidation of this charge-transfer species by electron transfer to the artificial redox acceptor will generate the oxidized enzyme in complex with $NADP^+$. Oxidation of the FAD will weaken the interaction with $NADP^+$, and it will be more readily released from the oxidized enzyme, allowing a further molecule of NADPH to bind. A similar mechanism for enhancing the rate of $NADP^+$ release through electron transfer to an artificial acceptor has been proposed for the FAD domain of human NR1 (*17*). In BM3 reductase, electron transfer to the FMN domain generates an enzyme species with blue semiquinone features (i.e., containing semiquinone FAD and semiquinone FMN), which is in complex with $NADP^+$. In this form of BM3, the rate of release of $NADP^+$ from the enzyme will be increased owing to the lack of charge transfer with the FAD. Thus, removal of the $FADH_2-NADP^+$ charge-transfer complex by inter-flavin electron transfer allows catalysis to proceed and is consistent with the lack of spectral signature for the $FADH_2-NADP^+$ charge-transfer complex in stopped-flow studies with BM3 reductase.

In previous studies with human CPR and neuronal nitric oxide synthase reductase, we presented evidence for a kinetic model that invokes two binding sites for coenzyme. This model explains the unusual dependence of the flavin reduction rate on the concentration of nicotinamide coenzyme (*28*, *30*). The model was extended recently to the single flavin enzyme FprA from *M. tuberculosis*, which is a homologue of adrenodoxin reductase (*29*). Although evidence for a second coenzyme-binding site in BM3 reductase was not found in stopped-flow studies of flavin reduction by NADPH, analysis of the reverse reaction revealed a complex dependence that is consistent with the presence of a second coenzyme-binding site. The same bipartite binding site for coenzyme appears therefore to exist in BM3 reductase. The kinetic scheme proposed (Figure 5) is consistent with the observed dependence of the rate of flavin oxidation on $NADP^+$ concentration. Differences in the kinetics of binding and release at the catalytic and regulatory sites in BM3 reductase and human CPR no doubt account for the lack of an unusual dependence of the flavin reduction rate on NADPH concentration in BM3 reductase (i.e., catalysis in the physiological direction). Likewise, the lack of an unusual dependence on coenzyme concentration in the C999A enzymes probably reflects altered kinetics for nicotinamide coenzyme exchange at one or both of the sites.

That the reduction of NAD^+ by the wild-type FAD domain or reduction of $NADP^+$ in the presence of 2′AMP exhibits a positive hyperbolic dependence on NAD^+ concentration provides additional evidence for the two-site model (Table 4). We infer that NAD^+ will bind weakly to the inhibitory site owing to the absence of the 2′-phosphate group. The 2′-phosphate group is a major determinant for the binding of NADPH in many nicotinamide-dependent enzymes, and the importance of this group in binding mammalian CPR has been demonstrated by Kasper's group (*38*, *39*). Weak binding at the inhibitory site will not interfere with the release of NADH from the catalytic site. Also, we suggest that, due to its smaller size, 2′AMP does not sterically hinder release of NADPH from the catalytic site when 2′AMP is bound at the regulatory site. Clearly, the kinetics of coenzyme exchange in BM3 reductase are complex, and they affect the rate of flavin oxidation/reduction in different ways. In human CPR, the dynamic properties of Trp-676, whose side chain is positioned over the isoalloxazine ring of the FAD, have also been shown to affect the kinetics of coenzyme exchange (*30*). This residue is conserved in BM3 reductase as Trp-1043 (Figure 1). Interplay between the dynamical properties of this tryptophan residue and the occupation of the regulatory site by coenzyme is likely to affect the kinetics of coenzyme release in the catalytic site. Although this interplay has been demonstrated with human CPR (*30*), the

role of Trp-1046 in coenzyme release needs to be explored in BM3 reductase by appropriate mutagenesis and kinetic studies.

Our mutagenesis study has indicated that the major role of Cys-999 is to enhance the rate of hydride transfer from NADPH to FAD. The origin of this enhancement is in the correct orientation of the NMN portion of the coenzyme with respect to the FAD and not in any thermodynamic perturbation as a result of altered reduction potential for the FAD. The formation of a stable charge-transfer $FADH_2-NADP^+$ species in the wild-type, but not C999A, FAD domain also suggests that Cys-999 plays a role in stabilizing the reduced enzyme$-NADP^+$ complex. That Cys-999 substantially enhances the rate of hydride transfer is concordant with the proposed role of Cys-630 in rat CPR. Kasper and colleagues have suggested that Cys-630 promotes hydride transfer from NADPH to FAD by correctly orientating the nicotinamide ring of NADPH and by stabilizing the formation of a transient carbocation on the nicotinamide following hydride transfer (*40*). Crystallographic studies of the wild-type and triad mutants of rat CPR have indicated that the three triad residues form a hydrogen-bonded network, which is disrupted on binding nicotinamide coenzyme and re-formed after $NADP^+$ release (*40*). The structural data are consistent with Cys-630 stabilizing a transient carbocation formed following hydride transfer to the flavin. The triad is also ideally positioned to facilitate proton transfer to the hydroquinone or semiquinone FAD: Ser-457 is hydrogen bonded to the flavin N5 atom. It seems likely that the corresponding triad in BM3 reductase is arranged similarly. Cysteine residues homologous to Cys-999 are conserved across the family of diflavin reductases, with the exception of human NR1 (Figure 1). In human NR1, the corresponding residue is Ala-549, and hydride transfer is fully rate-limiting ($\sim$1 s^{-1} at 25 °C compared to 237 s^{-1} for wild-type BM3 reductase at 5 °C) (*17*). Studies with the A549C mutant FAD domain of human NR1 indicate that it has an elevated rate of steady-state reductase activity with ferricyanide (R. D. Finn, A. W. Munro, M. J. Paine, and N. S. Scrutton, unpublished data), suggesting enhanced rates of hydride transfer. Our kinetic studies with BM3 reductase and NADH also highlight the importance of the 2′-phosphate moiety of NADPH in the binding and correct orientation of the NMN region of the coenzyme with respect to the flavin isoalloxazine ring.

In stopped-flow studies, the rate constant for the slower second phase observed at 450 nm during reduction of the flavins in BM3 reductase by nicotinamide coenzyme is less than the turnover number for cytochrome *c* reduction (Tables 1 and 3). Cytochrome *c* accepts electrons from the FMN domain, and thus the second phase is unlikely to represent inter-flavin electron transfer. The second slow phase observed in stopped-flow studies probably reflects disproportionation of the enzyme (i.e., a displacement of the equilibrium distribution of enzyme species toward further reduction of the FAD), as seen for the reductase domains of NOS and CPR (*20*, *28*). Indeed, the rate of inter-flavin electron transfer in BM3 reductase is considered to be rapid (*18*). This is also consistent with our inability to observe a $FADH_2-NADP^+$ charge-transfer intermediate in BM3 reductase, since it decays rapidly owing to the fast rate of inter-flavin electron transfer. In this respect BM3 reductase appears to differ from mammalian CPR enzymes, since our recent studies have shown that the inter-flavin electron transfer in human CPR is considerably slower (55 s^{-1}) than would be expected on the basis of thermodynamics and the relatively short distance ($\sim$4 Å) between the flavins observed in the structure of the rat enzyme (3). Tollin and co-workers have also shown using flash photolysis methods that internal electron transfer in mammalian CPR is relatively slow, in agreement with our studies using temperature-jump relaxation methods (*41*).

Concluding Remarks. Sequence alignments indicate that BM3 reductase is related to mammalian CPR and other eukaryotic diflavin reductases. Cys-999, one component of a triad also comprising Asp-1044 and Ser-830, enhances hydride transfer to FAD and stabilizes the binding of $NADP^+$ to the 2-electron-reduced FAD domain. Removal of electrons from the FAD domain by rapid internal electron transfer to the FMN in BM3 reductase facilitates the release of $NADP^+$ by destabilizing the enzyme$-NADP^+$ charge-transfer complex. BM3 reductase and mammalian CPR are structurally related, but the kinetics of hydride transfer and inter-flavin electron transfer in BM3 reductase are considerably faster compared with the mammalian enzymes. BM3 reductase can bind two coenzyme molecules. In the reverse reaction this gives rise to an unusual dependence of the flavin oxidation rate on $NADP^+$ concentration. This kinetic behavior indicates that the bipartite binding site for the nicotinamide coenzyme observed in rat CPR is conserved in BM3 reductase, and this might present opportunities for regulating the activity of BM3 reductase in the cell.

REFERENCES

1. Munro, A. W., and Lindsay, J. G. (1996) *Mol. Microbiol. 20*, 1115−1125.
2. Iyanagi, T., and Mason, H. S. (1973) *Biochemistry 12*, 2297−2308.
3. Wang, M., Roberts, D. L., Paschke, R., Shea, T. M., Masters, B. S. S., and Kim, J.-J. P. (1997) *Proc. Natl. Acad. Sci. U.S.A. 94*, 8411−8416.
4. Narhi, L. O., and Fulco, A. J. (1987) *J. Biol. Chem. 262*, 6683−6690.
5. Narhi, L. O., Wen, L. P., and Fulco, A. J. (1988) *Mol. Cell. Biochem. 79*, 63−71.
6. Noble, M. A., Miles, C. S., Chapman, S. K., Lysek, D. A., Mackay, A. C., Reid, G. A., Hanzlik, R. P., and Munro, A. W. (1999) *Biochem. J. 339*, 371−379.
7. Ravichandran, K. G., Boddupalli, S. S., Hasemann, C. A., Peterson, J. A., and Deisenhofer, J. (1993) *Science 261*, 731−736.
8. Li, H. Y., and Poulos, T. L. (1997) *Nat. Struct. Biol. 4*, 140−146.
9. Ost, T. W. B., Miles, C. S., Munro, A. W., Murdoch, J., Reid, G. A., and Chapman, S. K. (2001) *Biochemistry 40*, 13421−13429.
10. Leclerc, D., Wilson, A., Dumas, R., Gafuik, C., Song, D., Watkins, D., Heng, H. H., Rommens, J. M., Scherer, S. W., Rosenblatt, D. S., and Gravel, R. A. (1998) *Proc. Natl. Acad. Sci. U.S.A. 95*, 3059−3064.
11. Griffith, O. W., and Stuehr, D. J. (1995) *Annu. Rev. Physiol. 57*, 707−736.
12. Paine, M. J. I., Garner, A. P., Powell, D., Sibbald, J., Sales, M., Pratt, N., Smith, T., Tew, D. G., and Wolf, C. R. (2000) *J. Biol. Chem. 275*, 1471−1478.
13. Munro, A. W., Noble, M. A., Robledo, L., Daff, S., and Chapman, S. K. (2001) *Biochemistry 40*, 1956−1963.
14. Iyanagi, T., Makino, N., and Mason, H. S. (1974) *Biochemistry 13*, 1701−1710.
15. Daff, S. N., Chapman, S. K., Turner, K. L., Holt, R. A., Govindaraj, S., Poulos, T. L., and Munro, A. W. (1997) *Biochemistry 36*, 13816−13823.
16. Wolthers, K., Basran, J., Munro, A. W., and Scrutton, N. S. (2003) *Biochemistry 42*, 3911−3920.
17. Finn, R. D., Basran, J., Roitel, O., Wolf, C. R., Munro, A. W., Paine, M. J. I., and Scrutton, N. S. (2003) *Eur. J. Biochem. 270*, 1164−1175.

18. Munro, A. W., Daff, S., Coggins, J. R., Lindsay, J. G., and Chapman, S. K. (1996) *Eur. J. Biochem. 239*, 403−409.
19. Guengerich, F. P., and Johnson, W. W. (1997) *Biochemistry 36*, 14741−14750
20. Gutierrez, A., Lian, L.-Y., Wolf, C. R., Scrutton, N. S., and Roberts, G. C. K. (2001) *Biochemistry 40*, 1964−1975.
21. Shen, A. L., Sem, D. S., and Kasper, C. B. (1999) *J. Biol. Chem. 274*, 5391−5398.
22. Govindaraj, S., and Poulos, T. L. (1997) *J. Biol. Chem. 272*, 7915−7921.
23. Miles, J. S., Munro, A. W., Rospendowski, B. N., Smith, W. E., McKnight, J., and Thomson, A. J. (1992) *Biochem. J. 288*, 503−509.
24. Daff, S., Sharp, R. E., Short, D. M., Bell, C., White, P., Manson, F. D. C., Reid, G. A., and Chapman, S. K. (1996) *Biochemistry 35*, 6351−6357.
25. Dutton, P. L. (1978) *Methods Enzymol. 54*, 411−435.
26. Murataliev, M. B., and Feyereisen, R. (1997) *Biochemistry 36*, 8401−8412.
27. Lee, H. J., Basran, J., and Scrutton, N. S. (1998) *Biochemistry 37*, 15503−15512.
28. Knight, K., and Scrutton, N. S. (2002) *Biochem. J. 367*, 19−30.
29. McLean, K. J., Scrutton, N. S., and Munro, A. W. (2003) *Biochem. J. 372*, 317−327.
30. Gutierrez, A., Paine, M., Wolf, C. R., Scrutton, N. S., and Roberts, G. C. K. (2002) *Biochemistry 41*, 4626−4637.
31. Stuehr, D. J. (1999) *Biochim. Biophys. Acta 1411*, 217−230.
32. Munro, A. W., Leys, D. G., McLean, K. J., Marshall, K. R., Ost, T. W. B., Daff, S., Miles, C. S., Chapman, S. K., Lysek, D. A., Moser, C. C., Page, C. C., and Dutton, P. L. (2002) *Trends Biochem. Sci. 27*, 250−257.
33. Lee, T.-R., Hsu, H.-P., and Shaw, G.-C. (2001) *J. Biochem. 130*, 569−574.
34. *Ralstonia metallidurans* homepage at the DOE microbial genomes web site: http://www.jgi.doe.gov/JGI_microbial/html/ralstonia/ralston_homepage.html.
35. Noble, M. A., Munro, A. W., Rivers, S. L., Robledo, L., Daff, S. N., Yellowlees, L. J., Shimizu, T., Sagami, I., Guillemette, J. G., and Chapman, S. K. (1999) *Biochemistry 38*, 16413−16418.
36. Murataliev, M. B., and Feyereisen, R. (2000) *Biochemistry 39*, 12699−12707.
37. Murataliev, M. B., and Feyereisen, R. (2000) *Biochemistry 39*, 5066−5074.
38. Sem, D. S., and Kasper, C. B. (1993) *Biochemistry 32*, 11539−11547.
39. Sem, D. S., and Kasper, C. B. (1993) *Biochemistry 32*, 11548−11558.
40. Hubbard, P. A., Shen, A. L., Paschke, R., Kasper, C. B., and Kim, J.-J. P. (2001) *J. Biol. Chem. 276*, 29163−29170.
41. Bhattacharyya, A. K., Lipka, J. J., Waskell, L., and Tollin, G. (1991) *Biochemistry 30*, 259−265.

BI034562H